Millennial changes in North American wildfire and soil activity over the last glacial cycle

Hubertus Fischer[1*], Simon Schüpbach[1], Gideon Gfeller[1], Matthias Bigler[1], Regine Röthlisberger[1], Tobias Erhardt[1], Thomas F. Stocker[1], Robert Mulvaney[2], Eric W. Wolff[3]

[1] Climate and Environmental Physics, Physics Institute & Oeschger Centre for Climate Change Research, University of Bern, Sidlerstrasse 5, 3012 Bern, Switzerland, hubertus.fischer@climate.unibe.ch

[2] British Antarctic Survey, Cambridge, U.K.

[3] Department of Earth Sciences, University of Cambridge, Cambridge, U.K.

Climate changes in the North Atlantic region during the last glacial cycle were dominated by the slow waxing and waning of the North American ice sheet as well as by intermittent Dansgaard-Oeschger (DO) events. However prior to the last deglaciation, little is known about the response of North American vegetation to such rapid climate changes and especially about the response of biomass burning, an important factor for regional changes in radiative forcing. Here we use continuous, high-resolution ammonium (NH_4^+) records derived from the NGRIP and GRIP ice cores to document both North American NH_4^+ background emissions from soils and wildfire frequency over the last 110,000 yr. Soil emissions increased on orbital timescales with warmer climate, related to the northward expansion of vegetation due to reduced ice-covered areas. During Marine Isotope Stage (MIS) 3 DO warm events, a higher fire recurrence rate is recorded, while

NH_4^+ soil emissions rose only slowly during longer interstadial warm periods, in line with slow ice sheet shrinkage and delayed ecosystem changes. Our results indicate that sudden warming events had little impact on NH_4^+ soil emissions and NH_4^+ aerosol transport to Greenland during the glacial but triggered a significant increase in the frequency of fire occurrence.

Wildfires represent an important driver in ecosystem development[1] and pyrogenic emissions of trace gases, black carbon and other aerosol components have a strong regional effect on the radiation balance and atmospheric chemistry[2]. A detailed understanding of the response of vegetation and wildfire activity to climate change is hampered by the relatively long timescales of ecosystem change and fire recurrence. Paleoclimate information can help in this regard, documenting a wide range of climate and environmental changes on orbital, millennial and decadal timescales.

During the last glacial cycle, the climate of the northern hemisphere was fundamentally altered as ice cover and sea level varied[3], impacting the areal extent of vegetation and its composition. On top of these slow changes, the North Atlantic region was characterized by rapid DO warmings, where temperatures in Greenland increased by 10-15°C in a few decades[4,5]. These events also had strong, far-field effects on boreal and tropical methane emissions[6], monsoon intensity[7] and dust emissions in Chinese desert areas[8,9]. However, there is little paleoclimate information available from North America (NA), especially at a resolution allowing the identification of DO events in continental, ice-free regions[10-14]. In particular, the continent-wide reconstruction of wildfire activity based on charcoal records does not extend beyond the last glacial/interglacial transition[1,15].

North American soil and wildfire signal in Greenland ice cores

Greenland ice cores can fill this gap because aerosol-transported NH_4^+ in the ice comes from NA soil emissions but (together with other pyrogenic aerosol tracers[16,17]) also from NA wildfire events[17,18]. Background NH_4^+ concentrations in Greenland are derived mainly from bacterial decomposition of nitrogen in NA soils[19], leading to a broad NH_4^+ summer maximum in Greenland ice[18,20]. On top of this mean annual cycle, very large peaks are detected during individual summers, caused by NA biomass burning events[21,22], also characterised by co-occurring peaks in fire-specific organic aerosol compounds[17,23]. These events exceed the NH_4^+ background by more than an order of magnitude and dominate the Greenland NH_4^+ budget in those years[18,20]. The imprint of these events is strongly dependent on atmospheric circulation at the time of the fire, which must be favourable for long-range transport from NA to Greenland. Accordingly, not all fire events are recorded in Greenland ice. However, averaged over a sufficient time period, ice core records can provide a reliable picture of relative changes in NA wildfire frequency[18]. When measured at high resolution, the NH_4^+ ice core record can provide the change in average background NH_4^+ from soil emissions, concentrations of fire events above this background and fire peak frequency (FPF).

In this study, Greenland NH_4^+ concentrations were measured in cm-resolution on the NGRIP ice core with our Continuous Flow Analysis[24,25] system and complemented by published data from the GRIP[18] ice core. The changes in these ice cores show essentially the same variations on millennial down to decadal timescales (Figures 2-4), proving that our records provide a reliable picture of NH_4^+ deposition in Greenland. Here we concentrate on the higher resolution NGRIP record, providing a continuous record from

10,000-110,000 yr before present (BP, where present is 1950) at annual resolution well into the last glacial (Figure 1).

The NH_4^+ ice concentration in Greenland represents a convolved signal of changes in emissions, transport and aerosol deposition. To go beyond previous attempts to interpret ice core aerosol records, we provide first-order reconstructions of the atmospheric aerosol concentration over the ice sheet and in the NA source region, the latter directly reflecting changes in NH_4^+ emissions (for details of the toolkit used for atmospheric aerosol reconstruction see Methods and Supplementary Information). In short, using recent NH_4^+ observations in Greenland snow and atmospheric aerosol, the effect of local deposition can be corrected for to translate snow concentration into atmospheric aerosol concentration over the ice sheet. Making first-order assumptions about past changes in lifetime/washout of NH_4^+ aerosols along its transport path, we derive an estimate of the aerosol concentration in the source region. To account for the uncertainty in our simple model, we performed sensitivity tests and rigorous error propagation. This includes the uncertainty in the deposition over the ice sheet, the transport time and atmospheric lifetime en route, providing upper and lower limits for our atmospheric reconstruction at the source (Figures 1-4).

The NGRIP NH_4^+ ice concentrations in Figure 1 show interannual variability larger than the average glacial/interglacial changes. Superimposed on this high-frequency variability are significant long-term variations. Throughout the record, pronounced positive outliers caused by biomass burning events can also be detected. The relative interannual variability is much more pronounced in extended warm periods (Figures 2-4 and S3), implying that fire and soil activity were not only higher but also more variable

in these periods. We will discuss the changes in NH_4^+ background soil emissions separately from the change in the frequency of fire peaks. To this end, we use the peak-insensitive running median in a 101-yr window to quantify changes in background concentrations at the source derived from soil emissions and use a robust outlier detection method (see Methods and Supplementary Information) to identify fire peaks in the source concentration, quantify their concentration above the corresponding background and calculate the FPF. Performing both positive and negative outlier detection relative to the running median, we can correct the positive outlier count for the small number of positive outliers, which, implied by statistics, occur in the distribution of annual concentrations but are actually derived from extraordinarily high soil emissions. Accordingly, we are confident that we essentially identify only fire events in our peak count.

Long-term changes in North American NH_4^+ soil emissions

The atmospheric aerosol reconstruction in Figure 1 demonstrates that on orbital timescales the relative changes in NH_4^+ background concentrations at the source are covariant with those in the ice. This shows that the long-term evolution of the NH_4^+ record is not controlled by transport and/or deposition effects but by source emission changes. The relative amplitudes of the observed variations are larger at the source than in the ice. The absolute amplitudes are dependent on the assumptions made for the change in atmospheric lifetime, however, the dependence of the temporal evolution in the relative changes in NH_4^+ emissions on these assumptions is small. In our best-guess reconstruction, the NGRIP NH_4^+ ice concentrations increased by a factor of 3-5 during the last glacial/interglacial transition but by a factor of ~10 in atmospheric aerosol concentrations at the source. Note that such a change is also seen in organic acid aerosol

components[23] and in NO_3^-[9], which are also of NA biogenic origin, but is opposite to that of sea salt or mineral dust aerosol[8,9]. During the glaciation into Marine Isotope Stage (MIS) 4 (70-80,000 yr ago), a NH_4^+ decline by approximately the same factor is observed.

This indicates that the NH_4^+ background concentrations from soil emissions slowly but strongly increase during long-lasting warm climate conditions. We attribute this to a general northward retreat of the ice sheet, enlarging the area of vegetation and soil formation but also bringing the NH_4^+ sources closer to Greenland. However, when reducing the atmospheric transport time in our reconstruction by 50%, transport changes still cannot explain the large glacial/interglacial variations. Accordingly, we mainly ascribe the long-term increase in soil emissions to the expansion of the NH_4^+ source area. A similar slow increase with warmer climate conditions is seen in the excess concentration from wildfires (Figures 2-4). This increase similarly reflects in part the increasing proximity of wildfires to Greenland but may also be affected by larger fire intensity due to greater fuel availability, the larger area of burnable vegetation or a change in fire type. In contrast, a direct impact of rapid temperature changes during DO events on NA soil emissions appears to be only of secondary importance, as the NH_4^+ background concentration at the source does not respond directly to the rapid DO warming. A delayed soil response in slowly thawing permafrost regions, however, cannot be excluded. Accordingly, the long-term changes in NH_4^+ and other biogenic aerosol tracers[23] can be regarded as an indirect indicator of ice sheet area variations, suggesting that the vegetated area in NA during MIS 5c and 5a was comparable to or slightly smaller than during the early Holocene. Vice versa, the vegetated area in MIS5b was slightly larger than in MIS 2-4. Taking our data at face value, soil NH_4^+ emissions, thus vegetated area, changed little during MIS2-4 (Figures 2&3).

Most of the stadial/interstadial variations seen in the source concentration are still within the uncertainty estimate of our reconstruction. However, the longest DO events (8, 12, 14 and 16) show a slow and delayed increase in average NH_4^+ source concentrations of up to a factor of about 2. In contrast, mineral dust (Ca^{2+}), sea salt (Na^+) (Figure 1) and SO_4^{2-} aerosol (Figures 2-4) show an immediate, much stronger decline during rapid warmings. The difference between NH_4^+ and SO_4^{2-} is especially noteworthy, as basic NH_3 is neutralized and transported in acidic SO_4^{2-} aerosol. This decoupling shows that it is not the availability of acidic SO_4^{2-} aerosols in the past atmosphere that controls the atmospheric NH_4^+ concentration in Greenland but rather total NH_4^+ emissions. We suggest the interstadial increase is again due to the areal shrinkage of the NA Ice Sheet (NAIS) during these very long Greenland Interstadials, as also imprinted in sea level reconstructions[3].

Stadial/interstadial changes in North American fire frequency

In contrast to the NH_4^+ background source concentrations from soil emissions, the FPF shows a clear and immediate response to most DO events during MIS3, with an approximate tripling of NH_4^+ peak frequency (Figure 2). Note that this increase may be even more pronounced for the longest DO events, where the smallest fire events cannot be detected anymore due to the concurrent increase in interannual variability in NH_4^+ source concentrations. As DO events are also times of higher annual ice layer thickness and resolution of our NH_4^+ record, we tested the validity of this result extensively (see Supplementary Information). All tests support the robustness of our results for FPF changes during MIS3.

A higher frequency of NH_4^+ peaks in parallel to DO warming may reflect an increase in the recurrence of large fire events but could also be attributed to more favourable transport conditions from NA to Greenland for these wildfire events. The general atmospheric flow pattern in MIS2-4 is largely controlled by the presence of the NAIS[26], which does not alter substantially during short DO events. Nevertheless, model experiments indicate that rapid stadial/interstadial reorganizations of atmospheric circulation over the North Atlantic occur over areas where sea ice changes[27,28]. Deuterium excess ice core observations during the Bølling-Allerød/Younger Dryas oscillation also suggest that rapid changes in sea ice led to an increased transport of more local atmospheric water vapour to Greenland[29]. However, the effect on NH_4^+ aerosol from continental sources remains unknown and other aerosol species such as mineral dust, sea salt and sulphate suggest a decline in aerosol transport to Greenland during interstadials. In view of the lack of any immediate response of the NH_4^+ background concentrations to such potential DO-related transport changes, which would affect soil and wildfire emissions similarly, the increased FPF during MIS3 interstadials is unlikely to be caused by improved transport to Greenland. Note that prior to DO20 (Figure 3), when NA glaciation was still only moderate, no clear increase in FPF can be found during DO events. However, the significantly higher interannual variability in the background NH_4^+ concentrations limits the quantitative detection of fire peaks during this period.

Independent evidence for a change in wildfire emissions and recurrence may come from the charcoal fire record. Despite the fact that the climate imprint of DO events was quite different in the northern and southern hemisphere[30], a global synthesis of charcoal concentrations suggests stronger interstadial wildfire emissions, especially for DO8 and

DO20[1], when our FPF indicates higher fire recurrence rates. Higher fire excess concentrations can also be detected in our record at those times, suggesting higher pyrogenic emissions. In contrast, higher fire activity at the end of MIS4, as suggested by the global charcoal synthesis, is not found in our NA fire frequency record. Unfortunately, no charcoal information during MIS3 exists for NA. The closest analogue is the rapid Bølling-Allerød (BA) warming, when the NAIS was still expanded[15]. The background NH_4^+ concentration at the source and the excess NH_4^+ concentration of fire peaks show a slow increase after the onset of the BA (Figure 4), which is (similar to MIS3 interstadials) delayed with respect to the rapid warming. The fire excess concentration stabilizes after about 500 yr into the BA and shows only a minor decrease during the Younger Dryas (YD), after which it slowly increases again. This temporal evolution of average NH_4^+ emissions for fire events from 15-10 kyr BP is overall in line with the NA charcoal flux record[15], despite the fact that our record is more sensitive to fires closer to Greenland. In contrast, our FPF record displays a temporal evolution quite different from that of charcoal peak density[15]. With the superior counting statistics and resolution of our FPF record compared to the NA charcoal density record, the FPF shows a rather immediate response to the BA climate variations and a clear YD minimum, similar to the FPF response during MIS3 stadials. The FPF change at the onset of the BA warming would be even more pronounced if small fire events were still detectable, however the increase in interannual variability prevents their identification. Again, the observed FPF change indicates a strong direct response of fire recurrence to rapid warmings, which appears to be most pronounced at the onset of the BA and at the end of the YD (Figure 4), potentially fuelled by an increased mortality of pre-existing vegetation in response to rapid climate change.

Our NGRIP record allows us to reconstruct both NH_4^+ background concentrations from NA soil emissions and wildfire frequency over the entire last glacial cycle, however, an aerosol tracer reflecting only biomass burning is desirable to also add specific information on fire emission strengths. While levoglucosan[16] shows high potential, it is not available at the same resolution as NH_4^+ records, crucial for quantifying fire recurrence rates. Our record shows that soil NH_4^+ emissions are higher for warm interglacial conditions due to the expansion of vegetation, while during glacial times NH_4^+ emissions are suppressed by the larger NA ice cover. The response of NH_4^+ soil emissions to rapid DO warmings is very limited and delayed, indicating that rapid temperature changes during DO events are not the controlling factor for NA nitrogen soil turnover, however the frequency for fire occurrence increases during rapid warmings.

Methods

NH_4^+ concentrations were measured on the NGRIP ice core on ice rods with a square cross section of about 10 cm^2 using our Continuous Flow Analysis (CFA) system[18,24] and complemented by previously published CFA data from the GRIP ice core[18]. Note that NH_4^+ measurements on discrete samples using classical ion chromatographic analysis are prone to NH_3 contamination by lab air and only CFA analysis provides the environment for reliable NH_4^+ measurements for the very low concentrations found in Greenland ice. Quantification of the NH_4^+ ice concentrations is based on a fluorimetric method using the reaction of NH_4^+ with o-phthaldialdehyde. The limit of detection of this method is 0.1 ng/g, the uncertainty of the measured concentration is always smaller than 0.4 ng/g[20,24]. The data are sampled in 1 mm resolution, however due to dispersion in the CFA system the true achievable resolution is 1.2 cm[25]. The NGRIP NH_4^+ raw data

were down-sampled to nominal annual averages according to the extended GICC05 age scale[31-33], the latter being based on multi-parameter layer counting down to 60 kyr BP and extended by a glaciological flow model for older ages. The nominal annual averages in NH_4^+ do not reflect annual means from one seasonal NH_4^+ minimum to the next but are defined by the available age scale. Moreover, layer counting based on NH_4^+ concentrations cannot be achieved throughout the record due to the maximum resolution of the CFA measurement and because the annual layer thickness is reduced for colder periods due to lower precipitation and generally declines with increasing depth due to glacier flow. This translates into a decreasing temporal resolution of the record with depth (Figure S4). Seasonal variations in the NGRIP NH_4^+ record can be clearly resolved for the late glacial/interglacial transition. The maximum resolution during DO events in MIS3 and the Last Glacial Maximum is 0.3-0.5 years and about one year for stadials in MIS3. In older ice only the warmest periods may allow for a maximum resolution of 1 year, while stadial resolutions are lower than 1 year (see also Supplementary Information).

To calculate the atmospheric aerosol concentration in Greenland from concentrations in the ice, we corrected for the effect of dry and accumulation-dependent wet deposition, using dry deposition velocities and scavenging ratios from literature values[34,35] and using an extended data set of spatial variations in mean NH_4^+ concentrations in shallow Greenland ice cores. Using the derived atmospheric concentration over the ice sheet we back-calculated the atmospheric aerosol concentration over the NA source region assuming an exponential decline from the source to the ice sheet dependent on transport time and atmospheric lifetime. To determine the recent NH_4^+ transport time to Greenland we calculated a back-trajectory climatology for the NEEM ice core site[36]

(assuming comparable transport conditions for NEEM and NGRIP) using only trajectories originating in the NA continental boundary layer and ending at NEEM. For the recent atmospheric lifetime of NH_4^+ en route we used the value by Dentener&Crutzen[19]. For the past we scaled the recent wet deposition (which is dependent on the total precipitation en route derived from the back-trajectory climatology) by the relative temporal change in accumulation rate at NGRIP. In order to account for the considerable uncertainties in this simple approach, we performed rigorous error propagation, including the uncertainty in the atmospheric lifetime en route as well as in the dry deposition velocity and the scavenging ratio over the ice sheet. Moreover, we tested the sensitivity of the results to changes in transport time (for details see Supplementary Information).

Finally, we separated background NH_4^+ concentrations derived from NA soil emissions from positive NH_4^+ outliers caused by NA biomass burning events. To quantify the background concentrations we used the running median in a 101 yr window as this robust measure is insensitive to a few years affected by wildfires. To identify the biomass burning events we used a threshold above the running median defined by three times the median of the absolute deviation from the median (MAD) in the 101 yr window. Using these identified peaks we were able to calculate peak frequencies. Assuming a symmetric lognormal distribution of the annual background concentrations around the median we were able to correct our peak count for the very small number of randomly occurring large peaks from soil emissions. This corrected peak count is always smaller than 20 per 201 year window and thus very similar (or in cold intervals even smaller) than the number of fire peaks unambiguously identified using other chemical

fire tracers[17]. Accordingly, with this approach we are confident that our corrected peak count is a reliable measure of fire peak frequency only.

The new annual resolution NH_4^+ concentrations and the data on spatial variations in average NH_4^+ ice concentrations in Greenland over the last centuries are available as supplementary tables of this publication.

GISP2 ion data[9] are available at:

ftp://ftp.ncdc.noaa.gov/pub/data/paleo/icecore/greenland/summit/gisp2/chem/iond.txt

GRIP NH4+ data are available at:

ftp://ftp.ncdc.noaa.gov/pub/data/paleo/icecore/greenland/summit/grip/chem/nh4.txt

NGRIP $\delta^{18}O$ data[4] and age scales for Greenland ice cores synchronized to the extended GICC05 age scale[37] are available at: http://www.iceandclimate.nbi.ku.dk/data

NGRIP ice core accumulation rates[5] are available at:

http://www.clim-past.net/10/887/2014/cp-10-887-2014-supplement.zip

The Red Sea sea level reconstruction[3] is available at:

http://www.nature.com/nature/journal/v491/n7426/full/nature11593.html

Charcoal compilation for North America over the last glacial/interglacial transition[15] is part of the Global Charcoal Data Base: https://www.ncdc.noaa.gov/paleo/impd/gcd.html. The compilation can be downloaded directly at : http://jennmarlon.info/papers/Marlon_etal_2012_PNAS_figure%20data.zip

References

1 Daniau, A.-L., Harrison, S. P. & Bartlein, P. J. Fire regimes during the Last Glacial. *Quat Sci Rev* **29**, 2918–2930, doi:10.1016/j.quascirev.2009.11.008 (2010).

2 McConnell, J. R. *et al.* 20th-Century Industrial Black Carbon Emissions Altered Arctic Climate Forcing. *Science* **317**, 1381-1384, doi:10.1126/science.1144856 (2007).

3 Grant, K. M. *et al.* Rapid coupling between ice volume and polar temperature over the past 150,000 years. *Nature* **491**, 744-747, doi:10.1038/nature11593 (2012).

4 North Greenland Ice Core Project members. High resolution climate record of the northern hemisphere reaching into the last interglacial period. *Nature* **431**, 147-151, doi:10.1038/nature02805 (2004).

5 Kindler, P. *et al.* Temperature reconstruction from 10 to 120 kyr b2k from the NGRIP ice core. *Climate of the Past* **10**, 887–902, doi:10.5194/cp-10-887-2014 (2014).

6 Baumgartner, M. *et al.* NGRIP CH4 concentration from 120 to 10 kyr before present and its relation to a $\delta^{15}N$ temperature reconstruction from the same ice core. *Clim. Past* **10**, 903-920, doi:10.5194/cp-10-903-2014 (2014).

7 Wang, Y. *et al.* Millennial- and orbital-scale changes in the East Asian monsoon over the past 224,000 years. *Nature* **451**, 1090-1093, doi:10.1038/nature06692 (2008).

8 Fischer, H., Siggaard-Andersen, M.-L., Ruth, U., Röthlisberger, R. & Wolff, E. Glacial/Interglacial changes in mineral dust and sea salt records in polar ice cores: sources, transport, deposition. *Rev Geophys* **45**, RG1002, doi:1010.1029/2005RG000192 (2007).

9 Mayewski, P. A. *et al.* Major features and forcing of high-latitude northern hemisphere atmospheric circulation using a 110,000-year-long glaciochemical series. *J Geophys Res* **102**, 26345-26366 (1997).

10 Jimenez-Moreno, G. *et al.* Millennial-scale variability during the last glacial in vegetation records from North America. *Quat Sci Rev* **29**, 2865–2881, doi:10.1016/j.quascirev.2009.12.013 (2010).

11 Asmerom, Y., Polyak, V. J. & Burns, S. J. Variable winter moisture in the southwestern United States linked to rapid glacial climate shifts. *Nature Geoscience* **3**, 114 - 117, doi:10.1038/NGEO754 (2010).

12 Sionneau, T. *et al.* Atmospheric re-organization during Marine Isotope Stage 3 over the North American continent: sedimentological and mineralogical evidence from the Gulf of Mexico. *Quat Sci Rev* **81**, 62-73, doi:10.1016/j.quascirev.2013.10.002 (2013).

13 Whitlock, C. & Bartlein, P. J. Vegetation and climate change in northwest America during the past 125 kyr. *Nature* **388**, 57-61 (1997).

14 Grimm, E. C., Jacobson, G. L., Watts, W. A., Hansen, B. C. S. & Maasch, K. A. A 50,000-year record of climate oscillations from Florida and its temporal correlation with the Heinrich events. *Science* **261**, 198-200 (1993).

15 Marlon, J. R. *et al.* Wildfire responses to abrupt climate change in North America. *Proceedings of the National Academy of Sciences* **106**, 2519–2524, doi:10.1073/pnas.0808212106 (2009).

16 Zennaro, P. *et al.* Fire in ice: two millennia of boreal forest fire history from the Greenland NEEM ice core. *Climate of the Past* **10**, 1905–1924, doi:10.5194/cp-10-1905-2014 (2014).

17 Savarino, J. & Legrand, M. High northern latitude forest fires and vegetation emissions over the last millennium inferred from the chemistry of a central Greenlabd ice core. *J Geophys Res* **103**, 8267-8279 (1998).
18 Fuhrer, K., Neftel, A., Anklin, M., Staffelbach, T., Legrand, M. High resolution ammonium ice core record covering a complete glacial-interglacial cycle. *J Geophys Res* **101**, 4147-4164 (1996).
19 Dentener, F. J. & Crutzen, P. J. A Three-Dimensional Model of the Global Ammonia Cycle. *Journal of Atmospheric Chemistry* **19**, 331-369 (1994).
20 Gfeller, G. *et al.* Representativeness of major ions measurements and seasonality derived from NEEM firn cores. *The Cryosphere* **8**, 1855–1870, doi:10.5194/tc-8-1855-2014 (2014).
21 Kehrwald, N. *et al.* Levoglucosan as a specific marker of fire events in Greenland snow. *Tellus B* **64**, 18196, 18110.13402/tellusb.v18164i18190.18196 (2012).
22 Jaffrezo, J.-L. *et al.* Biomass burning signatures in the atmosphere of central Greenland. *J Geophys Res* **103**, 31067-31078 (1998).
23 Legrand, M. & De Angelis, M. Light carbolyxic acids in Greenland ice: A record of past forest fires and vegetation emissions from the boreal zone. *J Geophys Res* **101**, 4129-4145 (1996).
24 Röthlisberger, R. *et al.* Technique for continuous high-resolution analysis of trace substances in firn and ice cores. *Environmental Science and Technology* **34**, 338-342, doi:10.1021/es9907055 (2000).
25 Kaufmann, P. *et al.* An improved Continuous Flow Analysis (CFA) system for high-resolution field measurements on ice cores. *Environmental Science & Technology* **42**, 8044-8050, doi:10.1021/es8007722 (2008).
26 Pausata, F. S. R., Li, C., Wettstein, J. J., Kageyama, M. & Nisancioglu, K. H. The key role of topography in altering North Atlantic atmospheric circulation during the last glacial period. *Climate of the Past* **7**, 1089–1101, doi:10.5194/cp-7-1089-2011 (2011).
27 Kageyama, M. *et al.* Glacial climate sensitivity to different states of the Atlantic Meridional Overturning Circulation: results from the IPSL model. *Climate of the Past* **5**, 551–570 (2009).
28 Zhang, X., Lohmann, G., Knorr, G. & Purcell, C. Abrupt glacial climate shifts controlled by ice sheet changes. *Nature* **512**, 290-294, doi:10.1038/nature13592 (2014).
29 Steffensen, J. P. *et al.* High-resolution Greenland ice core data show abrupt climate change happens in few years. *Science* **321**, 680-684, doi:10.1126/science.1157707 (2008).
30 EPICA community members. One-to-one coupling of glacial climate variability in Greenland and Antarctica. *Nature* **444**, 195-198 (2006).
31 Wolff, E. W., Chappellaz, J., Blunier, T., Rasmussen, S. O. & Svensson, A. Millennial-scale variability during the last glacial: The ice core record. *Quat Sci Rev* **29**, 2828–2838, doi:10.1016/j.quascirev.2009.10.013 (2010).
32 Rasmussen, S. O. *et al.* A new Greenland ice core chronology for the last glacial termination. *J Geophys Res* **111**, D06102, doi:06110.01029/02005JD006079 (2006).
33 Svensson, A. *et al.* A 60 000 year Greenland stratigraphic ice core chronology. *Climate of the Past* **4**, 47-57 (2008).
34 Bergin, M. H. *et al.* The contributions of snow, fog, and dry deposition to the summer flux of anions and cations at Summit, Greenland. *J Geophys Res* **100**, 16275-16288 (1995).

35 Davidson, C. I., Bergin, M. H. & Kuhns, H. D. in *Chemical exchange between the atmosphere and polar snow* Vol. 43 *NATO ASI Series* (eds E.W. Wolff & Bales R.C.) 275-306 (Springer Verlag, 1996).
36 NEEM community members. Eemian interglacial reconstructed from a Greenland folded ice core. *Nature* **493**, 489-494, doi:10.1038/nature11789 (2013).
37 Seierstad, I. K. *et al.* Consistently dated records from the Greenland GRIP, GISP2 and NGRIP ice cores for the past 104 ka reveal regional millennial-scale $\delta^{18}O$ gradients with possible Heinrich event imprint. *Quat Sci Rev* **106**, 29-46, doi:10.1016/j.quascirev.2014.10.032 (2014).
38 Rasmussen, S. O. *et al.* A stratigraphic framework for abrupt climatic changes during the Last Glacial period based on three synchronized Greenland ice-core records: refining and extending the INTIMATE event stratigraphy. *Quat Sci Rev* **106**, 14-28, doi:10.1016/j.quascirev.2014.09.007 (2014).

Correspondence and requests for materials should be addressed to HF (hubertus.fischer@climate.unibe.ch).

Acknowledgments

The authors of this paper are indebted to the late Dietmar Wagenbach, who contributed to and inspired this research in numerous discussions. This paper has also greatly benefitted from the Sir Nicholas Shackleton fellowship, Clare Hall, University of Cambridge, U.K., awarded to HF in 2014. The Division for Climate and Environmental Physics, Physics Institute, University of Bern acknowledges the long-term financial support of ice core research by the Swiss National Science Foundation (SNSF) and the Oeschger Centre for Climate Change Research. EW is supported by a Royal Society professorship. NGRIP is directed and organized by the Department of Geophysics at the Niels Bohr Institute for Astronomy, Physics and Geophysics, University of Copenhagen. It is supported by funding agencies in Denmark (SNF), Belgium (FNRS-CFB), France (IPEV and INSU/CNRS), Germany (AWI), Iceland (RannIs), Japan (MEXT), Sweden (SPRS), Switzerland (SNSF) and the USA (NSF, Office of Polar Programs).

Author contributions

M.B. and R.R. performed the CFA measurements in the field at NGRIP and together with S.S. carried out raw data analysis. H.F. developed the time series analysis approach and together with R.M. and E.W. the concept for reconstruction of atmospheric concentrations. G.G. provided back trajectory analysis used in the transport model, T.E. contributed to the deposition model. All authors discussed the results and contributed to the interpretation and to the manuscript, which was written by H.F.

Competing financial interests

The authors declare no competing financial interests.

Figure Captions:

Figure 1: Climate and environmental changes recorded in Greenland ice cores – a sea salt (Na^+) and mineral dust (Ca^{2+}) aerosol concentrations in the GISP2 ice core; **b** stable water isotope temperature proxy in the NGRIP ice core[4] ($\delta^{18}O$ expressed in ‰ with respect to Vienna Standard Mean Ocean Water); **c** annual NH_4^+ concentration in the NGRIP ice core (grey) together with the 101 yr running median (orange) representing background concentrations; **d** atmospheric background NH_4^+ aerosol concentrations over the ice sheet (orange), together with its uncertainty band (light blue); **e** atmospheric background NH_4^+ aerosol concentration at the NA source from soil emissions (orange), together with its uncertainty band (light blue); **f** the atmospheric aerosol lifetime in days (black) controlled by the change in precipitation rate[5]; **g** relative sea level reconstruction based on Red Sea sediments (dark blue) together with its 95% confidence band (grey)[3]. All ice core derived data are displayed on the model extended GICC05 age scale[37], the sea level reconstruction is given on its own age scale.

Figure 2: High-resolution records of NH_4^+ soil emissions and wildfire activity in NA during MIS3 – a fire event concentrations (red dots) at the source in excess of the background concentrations. The grey line indicates the detection threshold for fire events; **b** atmospheric background NH_4^+ aerosol concentration from soil emissions at the NA source (101 yr running median, orange) together with its uncertainty band (light blue); **c** NH_4^+ background ice concentration in the NGRIP (101 yr running median, light orange) and the GRIP ice cores[18] (55 cm averages, grey); **d** DO variability in the NGRIP stable water isotope proxy during MIS3[5]; **e** SO_4^{2-} concentration in the GISP2 ice core[9]; **f** corrected fire peak frequency (FPF, purple) per 201 yr window. Warm Greenland Interstadials (GI) are indicated by numbers[38], cold stadials by light blue bars.

Figure 3: High-resolution records of NH_4^+ soil emissions and wildfire activity in NA during MIS4 and MIS5b - a-f same as in Figure 2.

Figure 4: High-resolution records of NH_4^+ soil emissions and wildfire activity in North America during the last glacial/interglacial transition - a-f same as in Figure 2; **g** NA charcoal influx compilation (brown) and **h** NA charcoal peak density (green) by Marlon et al.[15] on their own age scale.

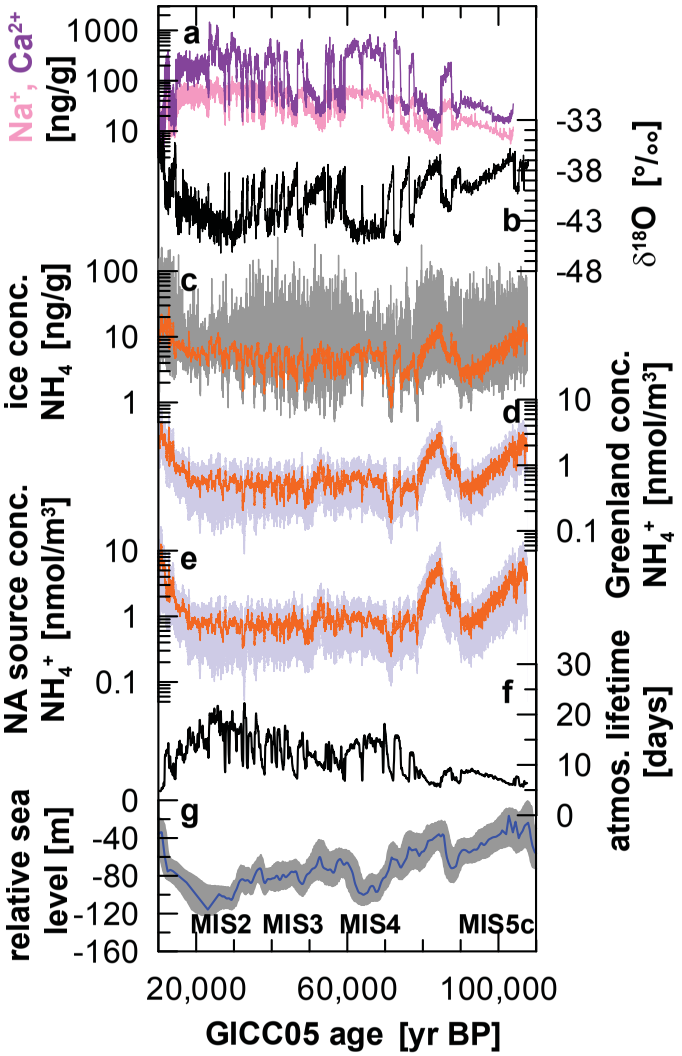
Na+, Ca2+ [ng/g]
1000
100
10
a
b
-33
-38
-43
-48
δ18O [‰]
ice conc. NH4 [ng/g]
100
10
1
c
d
10
1
0.1
Greenland conc. NH4+ [nmol/m3]
NA source conc. NH4+ [nmol/m3]
10
1
0.1
e
f
30
20
10
0
atmos. lifetime [days]
relative sea level [m]
0
-40
-80
-120
-160
g
MIS2
MIS3
MIS4
MIS5c
20,000
60,000
100,000
GICC05 age [yr BP]

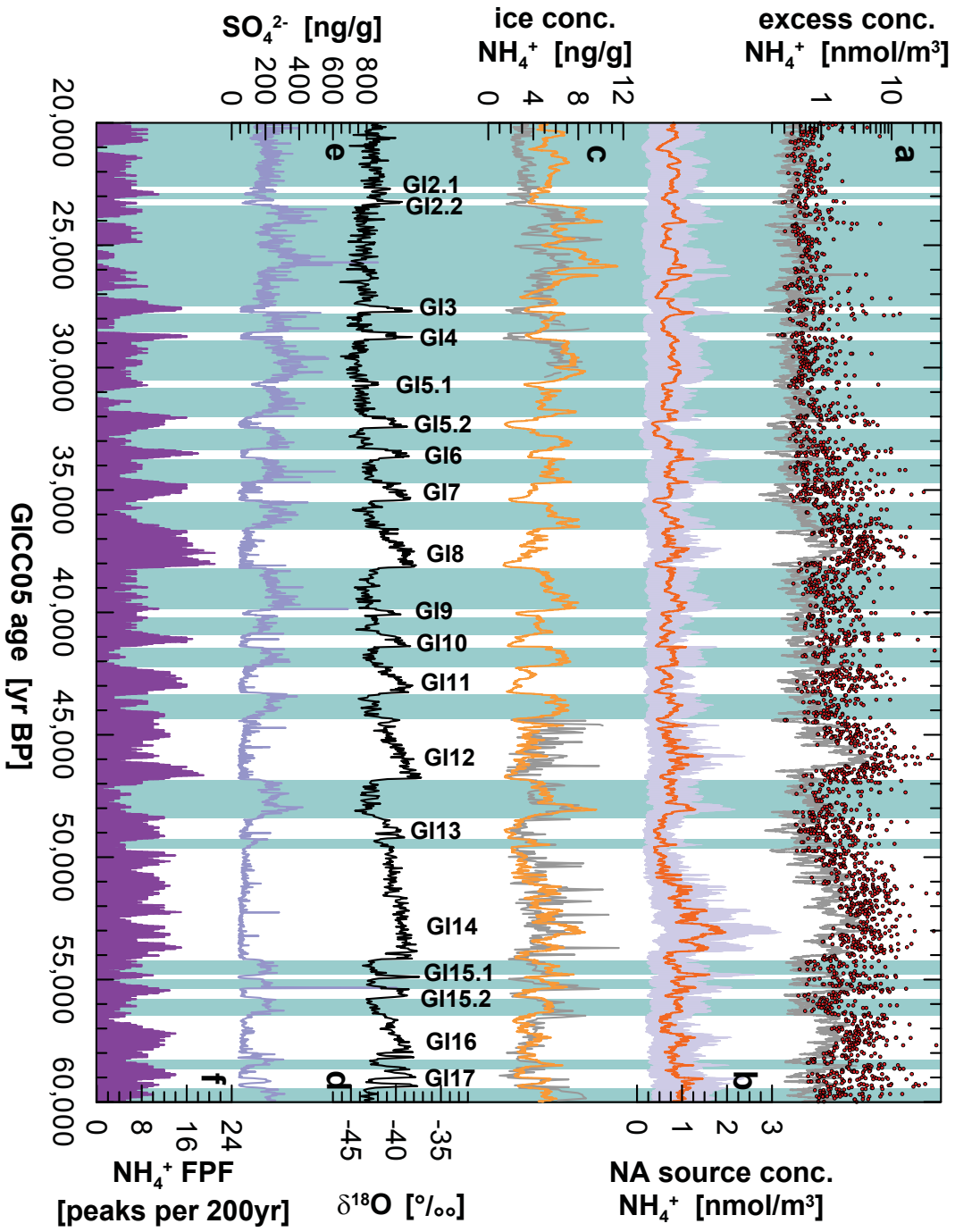
SO4 2- [ng/g]
ice conc. NH4+ [ng/g]
excess conc. NH4+ [nmol/m3]
GICC05 age [yr BP]
GI2.1
GI2.2
GI3
GI4
GI5.1
GI5.2
GI6
GI7
GI8
GI9
GI10
GI11
GI12
GI13
GI14
GI15.1
GI15.2
GI16
GI17
NH4+ FPF [peaks per 200yr]
δ18O [°/oo]
NA source conc. NH4+ [nmol/m3]

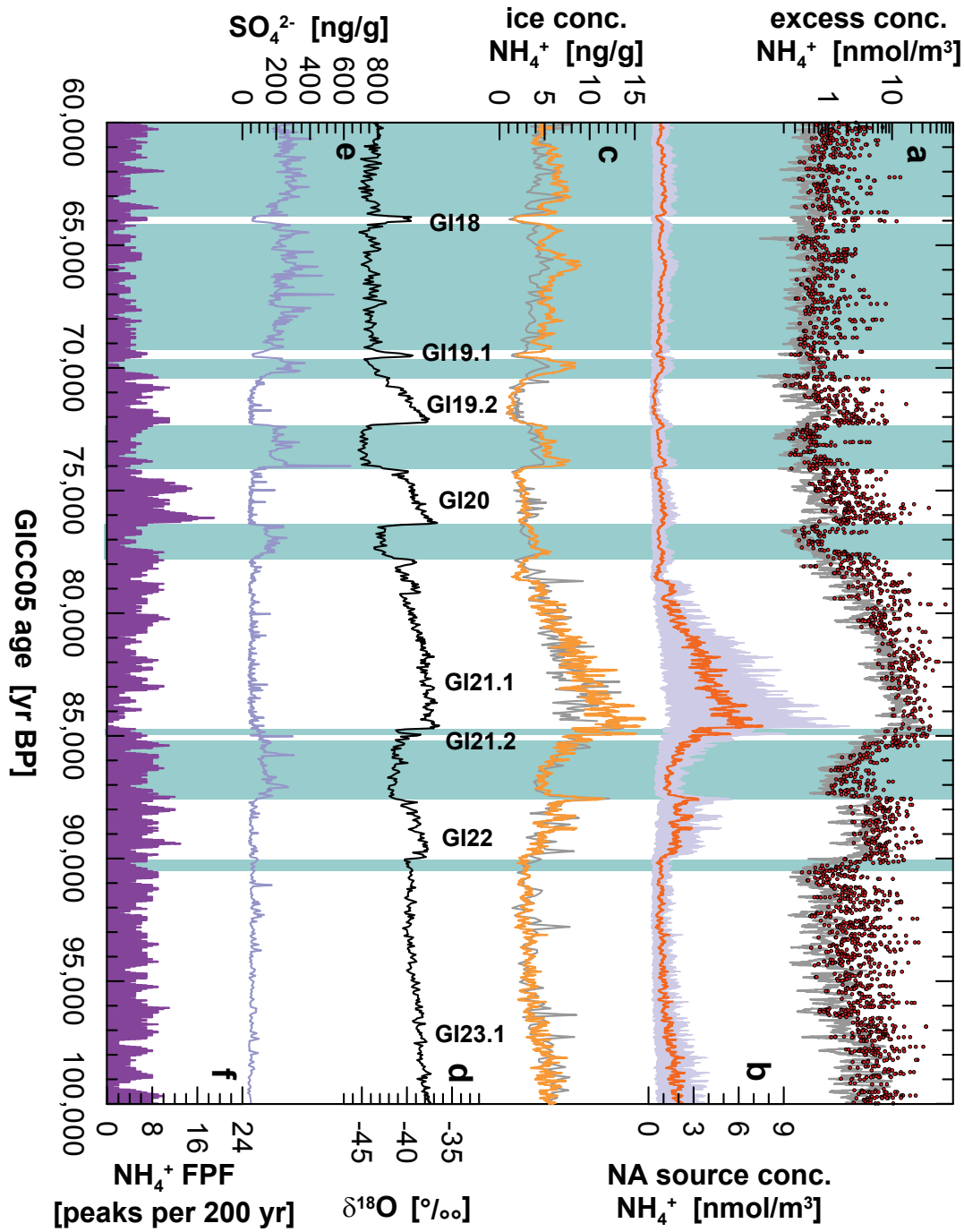
excess conc.
NH4+ [nmol/m3]
ice conc.
NH4+ [ng/g]
SO4 2- [ng/g]
a
b
c
d
e
f
GI18
GI19.1
GI19.2
GI20
GI21.1
GI21.2
GI22
GI23.1
GICC05 age [yr BP]
NA source conc.
NH4+ [nmol/m3]
δ18O [°/oo]
NH4+ FPF
[peaks per 200 yr]

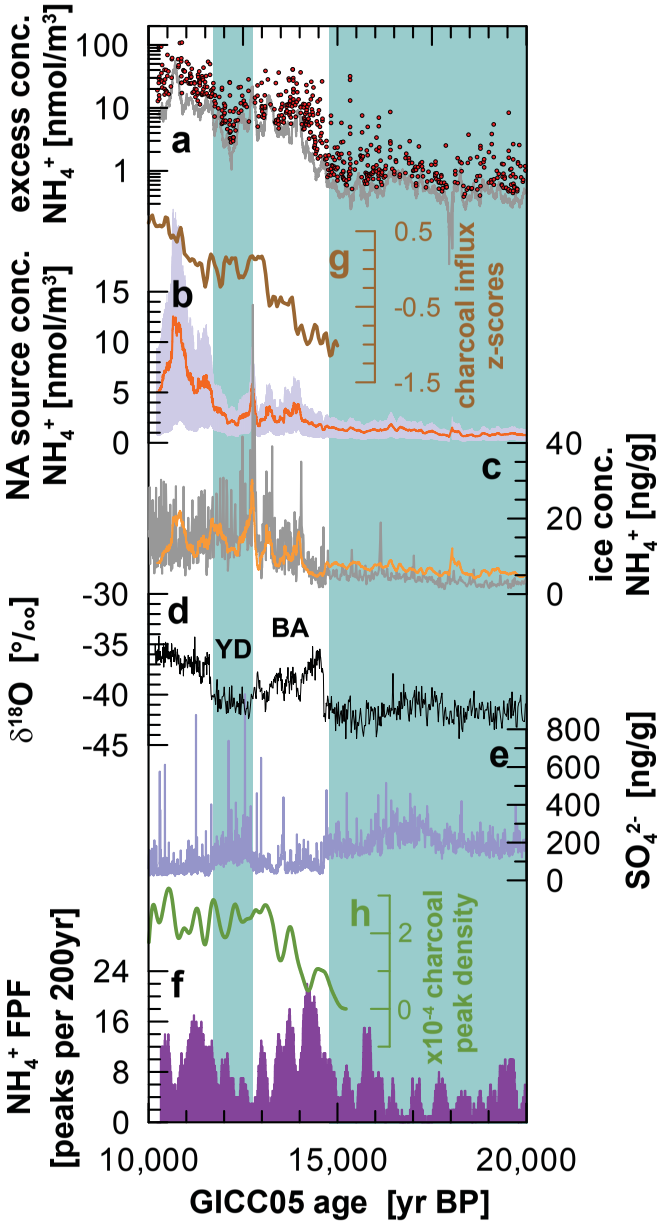
excess conc. NH_4^+ [nmol/m³]
100
10
1
a
NA source conc. NH_4^+ [nmol/m³]
15
10
5
0
b
g
0.5
-0.5
-1.5
charcoal influx z-scores
c
40
20
0
ice conc. NH_4^+ [ng/g]
$\delta^{18}O$ [‰]
-30
-35
-40
-45
d
YD
BA
e
800
600
400
200
0
SO_4^{2-} [ng/g]
NH_4^+ FPF [peaks per 200yr]
24
16
8
0
f
h
2
0
x10⁻⁴ charcoal peak density
10,000
15,000
20,000
GICC05 age [yr BP]